A Nanotechnology Pathway to Arresting Phase Separation in Soft Nanocomposites[a]

José A. Pomposo*, Alaitz Ruiz de Luzuriaga, Iñaki García, Agustín Etxeberria, Juan Colmenero

_____

J. A. Pomposo
Centro de Física de Materiales (CSIC, UPV/EHU) - Materials Physics Center, Paseo Manuel de Lardizabal 5, 20018 San Sebastián, Spain, and IKERBASQUE - Basque Foundation for Science, Alameda Urquijo 36, 48011 Bilbao, Spain
E-mail: josetxo_pomposo@ehu.es

A. Ruiz de Luzuriaga, I. Garcia
Departamento de Nuevos Materiales, Cidetec-Foundation, Paseo Miramón 196, 20009 San Sebastián, Spain

A. Etxeberria
Departamento de Ciencia y Tecnología de Polímeros, Universidad del País Vasco (UPV/EHU), Paseo Manuel de Lardizabal 3, 20018 San Sebastián, Spain

J. Colmenero
Donostia International Physics Center, Paseo Manuel de Lardizabal 4, 20018 San Sebastián, Spain, Centro de Física de Materiales (CSIC, UPV/EHU) - Materials Physics Center
Paseo Manuel de Lardizabal 5, 20018 San Sebastián, Spain, and Departamento de Física de Materiales, Universidad del País Vasco (UPV/EHU), Apartado 1072, 20800 San Sebastián, Spain

_____

Direct observation of the miscibility improving effect of ultra-small polymeric nanoparticles (radius ~4 nm) in model systems of soft nanocomposites is reported. We have found thermodynamically arrested phase separation in classical poly(styrene) (PS) / poly(vinyl methyl ether) blends when PS linear-chains were totally replaced by ultra-small, single-chain PS nanoparticles as determined by thermo-optical microscopy measurements. Partial arrested phase-splitting on heating was observed when only some of the PS chains were replaced by unimolecular PS nanoparticles leading to a significant increase of the lower critical solution temperature (LCST) of the system (up to 40 ºC at 15 vol. % nanoparticle content). Atomic

force microscopy and rheological experiments support these findings. Thermodynamic arrest of the phase separation process induced by replacement of linear-polymer-chains by unimolecular-polymer-nanoparticles could have significant implications for industrial applications requiring soft nanocomposite materials with excellent nanoparticle dispersion in a broad temperature range.

Introduction

Nanoparticles are currently ubiquitous in the nanotechnology arena showing a great impact in organic photovoltaics,[1] nanophotonics,[2] catalysis,[3] drug delivery,[4] and nanomedicine,[5] among other several fields.[6] A strong effort has been devoted in recent years to the efficient and shape-controlled synthesis of metallic, metal oxide and semiconducting (quantum dot) hard nanoparticles (HNPs). It is now well-established that HNP surface properties are mainly determined by chemical composition, surface chemistry (hydrophobic/hydrophilic balance), shape, size, porosity, roughness, and compositional heterogeneity.[7] Even when the progress in this field has been astonishing, highly-dense HNPs are sometimes far from ideal when employed in conjunction with soft matter (e.g. biomacromolecules). Compared to classical HNPs, the multi-gram synthesis of well-defined unimolecular polymeric nanoparticles in the sub-20 nm size range has been elusive until recently. The pioneering work of Hawker´s group[8] opened the way to new and highly efficient synthetic routes to monodisperse, ultra-small (radius < 5 nm) soft nanoparticles (SNPs).[9-16] The rich phase behavior of nanocomposites containing HNPs has been investigated by combining computer simulations,[17,18] theory[19-22] and experiment.[23, 24] Conversely, the miscibility (i.e. homogeneity at the nanoscale) behavior of soft nanocomposites consisting on unimolecular SNPs dispersed in a conventional polymer matrix remains largely unexplored, even if mimicking Nature´s soft nanocomposites is currently of great interest. Most thermodynamic (i.e. homogeneity) and rheological (i.e. dynamics) data correspond to simple blends of

intramolecular cross-linked polystyrene (PS)-nanoparticles dispersed in a matrix of PS linear-chains, displaying interesting non-Einstein viscosity behaviour.[25, 26] Also computer simulations[27, 28] and several theoretical approaches[26, 29] have focused on this kind of "athermal" systems as the simplest model of soft nanocomposites. Very recently, a theory describing the phase behaviour of compressible, weakly interacting soft nanocomposites has been introduced by relaxing the common HNP assumption and taking into account the presence of weak, enthalpic interactions between components.[30] In brief, an expression for the free energy of the system (F_m) was derived by accounting for ideal, combinatorial contributions (F_m^{co}), nonideal nanoparticle/nanoparticle interactions (F_m^{np-np}), the interaction energy between components (F_m^{int}) and stretching effects induced by the presence of the SNPs (F_m^{np-p}):

$$F_m = F_m^{co} + F_m^{np-np} + F_m^{\text{int}} + F_m^{np-p} \qquad (1)$$

Interestingly, a rich variety of phase diagrams have been predicted for soft nanocomposites depending on polymer and SNP size, SNP rigidity, polymer/SNP interaction energy and blend composition.[30] Although still very primitive for treating complex, soft bionanocomposites involving strong specific interactions such as hydrogen bonding or electrostatic interactions, this predictive theory allows one to compare the phase behavior of binary polymer blends (e.g. polyA / polyB) to that of the corresponding soft nanocomposites (e.g. polyA / polyB-SNP). In this sense, an excellent, canonical model system beyond the athermal case is that composed of blends of poly(vinyl methyl ether) (PVME) (i.e. polyA) and PS (i.e. polyB) displaying lower critical solution temperature (LCST) type phase behavior in a really accessible temperature range.[31-33] We have selected this simple system to investigate a promising Nanotechnology pathway to arresting phase separation in soft nanocomposites through replacement of linear chains by unimolecular nanoparticles.

In this communication we present the first experimental evidence of arrested phase separation in weakly interacting soft nanocomposites involving ultra-small, single-chain polymeric nanoparticles. We have found total (or partial) arrested phase separation for binary PVME/PS-SNPs (or ternary PVME/PS/PS-SNPs) nanocomposites by a combination of thermo-optical (micro-size resolution), AFM (nano-size resolution) and rheological (bulk) measurements. These striking experimental results can be rationalized by means of an appropriate thermodynamic theory for soft nanocomposites involving ultra-small polymeric nanoparticles. To the best of our knowledge, this is the first report of complete arrest of the phase separation process induced by replacement of linear-polymer-chains by unimolecular-polymer-nanoparticles (i.e. by a purely Nanotechnology pathway). The deep impact of this finding is significant, since as usually claimed: "obtaining the optimum properties for nanocomposites will usually require excellent dispersion of the nanoparticles".[24]

Experimental Part

Monodisperse PS samples of high molecular weight, M_w = 65 kDa and M_w = 284 kDa were supplied by Fluka. PVME was purchased from Scientific Polymer Products, M_w = 90 kDa, and PS of lower molecular weight was purchased from Aldrich, M_w = 35 kDa. PS-SNPs with a nanoparticle radius of 4 ± 1 nm, as determined by dynamic light scattering (Beckman Coulter N5) and AFM (Molecular Imaging PicoPlus) measurements, were synthesized by intramolecular "click" coupling from a poly(styrene$_{\mathbf{x}}$-co-azidomethyl styrene$_{\mathbf{y}}$-co-2-methyl-acrylic acid 3-trimethylsilanyl-prop-2-ynyl ester$_{\mathbf{z}}$) precursor (molar fraction of monomers: **x** = 0.84, **y** = 0.075 and **z** = 0.076; molecular weight, M_w = 55 kDa; polydispersity index, PDI = 1.24) using reported "click" chemistry procedures.[12, 16] Nanoparticle composition (H^1-NMR spectroscopy): content of styrene ~92.4 mol%, content of triazole cross-linking units ~7.3 mol%. Soft nanocomposite thin films (PVME/PS-SNP and PVME/PS/PS-SNP) were prepared by spin-coating the corresponding 5 wt. % toluene solutions over glass substrates (or

mica for selected AFM measurements) and dried under vacuum at 50 ºC until constant weight (typical thickness ~ 350 nm). Thermo-optical measurements were performed in a LEICA DM 400M microscope equipped with a LINKAM THMS600 hot plate and a LINKAM TMS94 temperature controller. For rheological measurements (TA Instruments AR2000ex), blends were prepared from toluene solutions after slowly removing of the solvent during 1 week and further drying under vacuum at 50 ºC for 4 days. Thermogravimetric measurements were performed in a TA Instruments TGA Q500 apparatus.

Results and Discussion

We have investigated what is the effect of replacing the PS linear-chains by ultra-small, single-chain PS-SNPs on the phase diagram of binary PVME/PS blends as a canonical model system. **Figure 1A and 1B** illustrate thermo-optical pictures for both PVME/PS blends and PVME/PS-SNP nanocomposites recorded at selected temperatures during heating at 1 ºC/min. As expected, phase-splitting (LCST-type) is clearly observed by thermo-optical microscopy (TOM) for the binary polymer blend at temperatures above T_c = 136 ºC (T_c being the cloud point temperature)[b] and the initial granular, phase-separated structure clearly evolved to well-defined biphasic morphology upon annealing at a temperature above T_c (see **Figure 1A**). Conversely, thermodynamically arrested phase separation was found when all PS linear-chains were replaced by ultra-small, single-chain PS-SNP (**Figure 1B**). Even after annealing at 260 ºC for 20 minutes, phase-splitting was absent. Annealing at higher temperatures was

[b] It is well-known that both the bimodal and spinodal curves merge at the critical point (*i.e.* $T_b = T_s$ at the critical point, being T_b and T_s the bimodal and spinodal temperatures, respectively). Under such circumstances the experimental cloud point temperature (T_c) is expected to be close to the actual LCST, *i.e.* $T_c / T_s \approx 1$.

complicated by the significant increase in the thermal degradation process of PVME as observed by the yellowing and emerging of small bubbles across the film (see Supporting

information, **Figure S1B**), but even in this case no sign of phase-splitting was apparent neither by TOM nor AFM (see **Figure S2**). It is worth noticing the excellent agreement between the lack of LCST behavior observed experimentally for PS-SNP/PVME nanocomposites and the corresponding predictions from the thermodynamic model for soft nanocomposites (equation 1),[30] in which complete miscibility above room temperature is predicted for PS-SNP with a radius lower than 5.7 nm (see **Figure 1C**). Vitrification of PS-SNP/PVME nanocomposites at low temperatures does prevent the UCST prediction to be experimentally ascertained. Further work is in progress to determine experimentally the precise placement of the miscibility boundary in the T *versus* R_p (nanoparticle radius) phase diagram. A complete thermodynamic analysis which is outside the scope of the present communication will be reported in due term.

Even more interesting and challenging was the case of partial replacement of PS linear-chains by PS-SNP leading to ternary soft nanocomposites. A comparison of the phase behavior for PVME/PS/PS-SNP nanocomposites (PS/PVME volume ratio = 1) as a function of the content of PS-SNP in the system is shown in **Figure 2TOM**. In this case, partial arrested phase-splitting on heating was observed by increasing the PS-SNP content in the ternary nanocomposite. Very similar behavior was observed by using PS of lower (35 kDa) or higher (284 kDa) molecular weight. AFM pictures of selected PVME/PS/PS-SNP nanocomposites annealed at $T = T_c + 10$ ºC for 30 minutes prior to rapid quenching are illustrated in **Figure 2AFM**. As a consequence of the presence of the PS-SNPs, a clear morphology change arising from improved compatibility and slow-down kinetics is observed when compared to the unfilled PVME/PS blends. A similar trend was clearly observed by TOM at a larger scale (see **Figure S3**). It is worth noticing that the progressive increase in T_c upon increasing PS-SNP content is in line with the totally arrested phase separation previously observed in the binary PVME/PS-SNP nanocomposites (**Figure 1B**) upon complete replacement of PS linear-chains by PS-SNPs.

The effect of phase-splitting on blend dynamics and hence rheological behavior has been highlighted by several theoretical, computer simulation and experimental works.[17, 19, 34-36] For quantitative studies of phase separation in binary PVME/PS blends[37] and ternary PVME/PS/HNPs nanocomposites,[35] the mean field theoretical approach of Ajji and Choplin[38, 39] has been demonstrated to be very reliable for determining phase separation temperatures from the T-dependence of the bulk elastic modulus (G´) and the bulk loss modulus (G´´) at small strain and very low shear rates (i.e. in the linear regime). The expression relating G´, G´´ and the phase separation temperature (T_s) is given by:

$$\Gamma \equiv \left[\frac{(G'')^2}{G'T}\right]^{2/3} \propto (\chi_s - \chi) \propto \left(\frac{1}{T_s} - \frac{1}{T}\right) \qquad (2)$$

where the classical 1/T dependence of the χ interaction parameter ($\chi = A + B/T$) is assumed. **Figure 3A-C** illustrate the corresponding Γ versus 1/T plot for PVME/PS/PS-SNP nanocomposites as a function of the PS-SNP volume fraction. T_s data extracted from the interception with the 1/T axis were in good agreement with T_c data determined by TOM for nanocomposite thin films (on average $T_c / T_s = 1.04 \pm 0.01$). In this sense, it is very instructive to compare the above experimentally determined phase separation temperatures (T_c, T_s) with the predictions from the compressible model (equation 1) extended to the case of ternary, weakly interacting all-polymer nanocomposites. For this case, equation 1 remains valid (the corresponding expressions for F_m^{co}, F_m^{np-np}, F_m^{int} and F_m^{np-p} are provided in the Supplementary Information) and the miscibility boundary in the T-composition diagram can be determined from the well-known spinodal condition:

$$\left|\begin{array}{cc} \dfrac{\partial^2 \Delta F_m}{\partial \phi_i^2} & \dfrac{\partial^2 \Delta F_m}{\partial \phi_i \, \partial \phi_j} \\ \dfrac{\partial^2 \Delta F_m}{\partial \phi_j \, \partial \phi_i} & \dfrac{\partial^2 \Delta F_m}{\partial \phi_j^2} \end{array}\right|_{T,P,\bar{\rho}} = \left(\frac{\partial^2 \Delta F_m}{\partial \phi_i^2}\right)_{T,P,\bar{\rho}} \left(\frac{\partial^2 \Delta F_m}{\partial \phi_j^2}\right)_{T,P,\bar{\rho}} - \left(\frac{\partial^2 \Delta F_m}{\partial \phi_i \, \partial \phi_j}\right)^2_{T,P,\bar{\rho}} = 0 \qquad (3)$$

A comparison of the theoretical and experimentally determined phase separation temperatures is given in **Figure 3D** for PVME/PS/PS-SNP nanocomposites (PS/PVME volume ratio = 1) as a function of the PS-SNP content, for polystyrenes differing in molecular weight. We have selected ternary compositions with a low content of PS-SNPs for which the theory is presumably more accurate, since the possibility of nanoparticle ordering at higher SNP volume fraction is not taken into account by the model. The precise placement of the experimental phase boundary for PVME/PS blends is known to be strongly affected by the molecular weight of the components.[31] A similar effect is observed in the experimental results shown in Figure 6 showing a better agreement between experiment and theory for PS of lower molecular weight (for PS of higher molecular weight kinetic effects presumably take place). Nevertheless, the observed experimental trend is well captured by the present thermodynamic model without the necessity of introducing any refinement. In this sense, the current model for ternary soft nanocomposites would be a good starting point for screening new systems in which the replacement of linear-polymer-chains by unimolecular-polymer-nanoparticles will lead to improved system homogeneity. Model parameters for several "commodity" polymers, from non-polar ones such poly(ethylene), poly(ethylenepropylene) or poly(isoprene) to relatively polar ones such as poly(acrylates), poly(methacrylates) or poly(carbonates) are readily available.[40, 41] Moreover, general avenues for the synthesis of well-defined unimolecular polymeric nanoparticles in the sub-20 nm size range are currently open.[8-16]

Conclusion

We have investigated by thermo-optical, AFM and rheological measurements the effect of the addition of ultra-small, PS-SPNs (R_p = 4 nm) on the phase behavior of PVME/PS blends

displaying LCST-type behavior in a really accessible temperature range. We have found thermodynamically arrested phase separation in PVME/PS-SNP nanocomposite thin films, when PS linear-chains were totally replaced by ultra-small, single-chain PS nanoparticles. When only some of the PS chains were replaced by unimolecular PS-SNPs, a significant increase in the LCST of the system was observed. Both AFM and TOM pictures illustrated a clear morphology change arising from improved compatibility and slow-down kinetics induced by the presence of the PS-SNPs. Arrest of the phase separation process induced by replacement of linear-polymer-chains by unimolecular-polymer-nanoparticles can be rationalized by means of a thermodynamic model for soft nanocomposites.[30] This new and promising Nanotechnology pathway could have significant implications for several industrial applications requiring nanocomposite materials with excellent nanoparticle dispersion across a broad temperate range (e.g. membranes, biosensors, biomimetic tissues, optical devices, etc.).

Acknowledgements: This work was supported by *MEC* (CIC NANOGUNE-CONSOLIDER Grant No. CSD2006-53) and *Basque Government* (INANOGUNE Project). A. R. thanks *Edurne Elorza* for technical assistance during synthesis and *Eider Begiristain* for nanoparticle size characterization.

Received: ((will be filled in by the editorial staff)); Revised: ((will be filled in by the editorial staff)); Published online: ((will be filled in by the editorial staff));

DOI: 10.1002/marc.201000720

Keywords: Ultra-small polymeric nanoparticles, Soft nanocomposites, Arrested phase separation, Size-dependent nano-effects

[1] J. E. Slota, X. Hea, W. T. S. Huck, *Nano Today* **2010**, *5*, 231.

[2] A. Alu, N. Engheta, *Nat. Photonics* **2008**, *2*, 307.

[3] R. A. Van Santen, *Acc. Chem. Res.* **2009**, *42*, 57.

[4] M. M.De Villiers, P. Aramwit, G. S. Kwon, *Nanotechnology in Drug Delivery*; Springer, New York, **2009**.

[5] M. A. Phillips, M. L. Granb, N. A. Peppas, *Nano Today* **2010**, *5*,143.

[6] R. Nagarajan, *Nanoparticles: Synthesis, Stabilization, Passivation, and Functionalization*; ACS Symposium Series, Vol. 996, **2008**; Chapter 1, pp 2-14.

[7] A. E. Nel, L. Madler, D. Velegol, T. Xia, E. M. V. Hoek, P. Somasundaran, F. Klaessig, V. Castranova, M. Thompson, *Nat. Mater.* **2009**, *8*, 543.

[8] E. Harth, B. Van Horn, V. Y. Lee, D. S. Germack, C. P. Gonzales, R. D. Miller, C. J. Hawker, *J. Am. Chem. Soc.* **2002**, *124*, 8653.

[9] J. Jiang, S. Thayumanavan, *Macromolecules* **2005**, *38*, 5886.

[10] A. E. Cherian, F. C. Sun, S. S. Sheiko, G. W. Coates, *J. Am. Chem. Soc.* **129**, *2007*, 11350.

[11] T. A. Croce, S. K. Hamilton, M. L. Chen, H. Muchalski, E. Harth, *Macromolecules* **2007**, *40*, 6028.

[12] A. Ruiz de Luzuriaga, N. Ormategui, H. J. Grande, I. Odriozola, J. A. Pomposo, I. Loinaz, *Macromol. Rapid Commun.* **2008**, *29*, 1156.

[13] C. T. Adkins, H. Muchalski, E. Harth, *Macromolecules* **2009**, *42*, 5786.

[14] E. J. Foster, E. B. Berda, E. W. Meijer, *J. Am. Chem. Soc.* **2009**, *131*, 6964.

[15] J. B. Beck, K. L. Killops, T. Kang, K. Sivanandan, A. Bayles, M. E.Mackay, K. L. Wooley, C. J. Hawker, *Macromolecules* **2009**, *42*, 5629.

[16] L. Oria, R. Aguado, J. A. Pomposo, J. Colmenero, *Adv. Mater.* **2010**, *22*, 3038.

[17] D. M. Hall, T. Lookman, S. Banerjee, *Chem. Eng. Sci.* **2009**, *64*, 4754.

[18] J. Y. Lee, G. A. Buxton, A. C. Balasz, *J. Chem. Phys.* **2004**, *121*, 5531.

[19] R. B. Thompson, V. V. Ginzburg, M. W. Matsen, A. C. Balazs, *Science* **2001**, *292*, 2469.

[20] V. V. Ginzburg, *Macromolecules* **2002**, *38*, 2362.

[21] E. Reister, G. H. Fredrickson, *J. Chem. Phys.* **2005**, *123*, 214903.

[22] J. B. Hooper, K. S. Schweizer, *Macromolecules* **2006**, *39*, 5133.

[23] F. Fenouillot, P. Cassagnau, J. C. Majesté, *Polymer* **2009**, *50*, 1333.

[24] D. R. Paul, L. M. Robeson, *Polymer* **2008**, *49*, 3187.

[25] M. E. Mackay, T. T. Dao, A. Tuteja, D. L. Ho, B. V. Horn, H. -C. Kim, C. J. Hawker, *Nature Mater.* **2003**, *2*, 762.

[26] M. E. Mackay, A. Tuteja, P. M. Duxbury, C. J. Hawker, B. V. Horn, Z. Guan, G. Chen, R. S. Krishnan, *Science* **2006**, *31*, 1740.

[27] H. Lin, F. Erguney, W. L. Mattice, *Polymer* **2005**, *46*, 6154.

[28] F. Erguney, H. Lin, W. L. Mattice, *Polymer* **2006**, *47*, 3689.

[29] J. A. Pomposo, A. Ruiz de Luzuriaga, A. Etxeberria, J. Rodríguez, *Phys. Chem. Chem. Phys.* **2008**, *10*, 650.

[30] A. Ruiz de Luzuriaga, H. J. Grande, J. A. Pomposo. *J. Chem. Phys.* **2009**, *130*, 084905.

[31] T. Nishi, T. K. Kwei, *Polymer* **1975**, *16*, 285.

[32] M. Shibayama, H. Yang, R. Stein, C. Han, *Macromolecules* **1985**,*18*, 2179.

[33] A. Etxeberria, M. Iriarte, M. J. Fernandez-Berridi, J. J. Iruin, *Polymer* **1994**, *35*, 2128.

[34] M. J. A. Hore, M. Laradji, *J. Chem. Phys.* **2007**, *126*, 244903.

[35] A. Gharachorlou, F. Goharpey, *Macromolecules* **2008**, *41*, 3276.

[36] Q. Fu, Q. Zhang, H. Yang, *Polymer* **2004**, *45*, 1913.

[37] K. E. Mabrouk, M. Bousmina, *Rheol. Acta* **2006**, *45*, 877.

[38] A. Ajji, L. Choplin, *Macromolecules* **1991**, *24*, 5221.

[39] G. H. Fredrickson, R. G. Larson, *J. Chem. Phys.* **1987**, *86*, 1553.

[40] A.-V. G. Ruzette, A. M. Mayes, *Macromolecules* **2001**, *34*, 1894.

[41] J. A. Gonzalez-Leon, A. M. Mayes, *Macromolecules* **2003**, *36*, 250.

Figure 1. Thermo-optical microscopy images of (A) binary PVME (M_w = 90 kDa) / PS (M_w = 65 kDa) blend and (B) binary PVME (M_w = 90 kDa) / PS-SNP (R_p = 4 nm, cross-linking degree = 7.3 mol%) soft nanocomposite thin films both for a PVME volume fraction of 0.7,

recorded at a scanning rate of 1 ºC/min. M_w denotes the weight-average molecular weight of the linear-polymer-chains and R_p is the average radius of the unimolecular nanoparticles. (C) Predicted miscibility diagram for binary PVME / PS-SNP soft nanocomposites as a function of R_p. Model parameters employed in the calculations were taken directly from reference [40]. Circles and triangles denote upper critical solution temperatures (UCST) and lower critical solution temperatures (LCST), respectively. Details about the thermodynamic model employed can be found in reference [30].

Fig. 1A

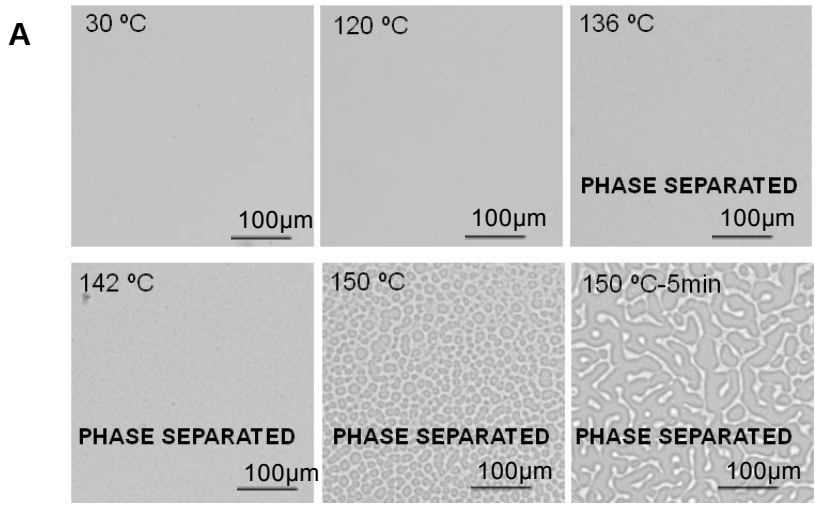

Fig. 1B

B

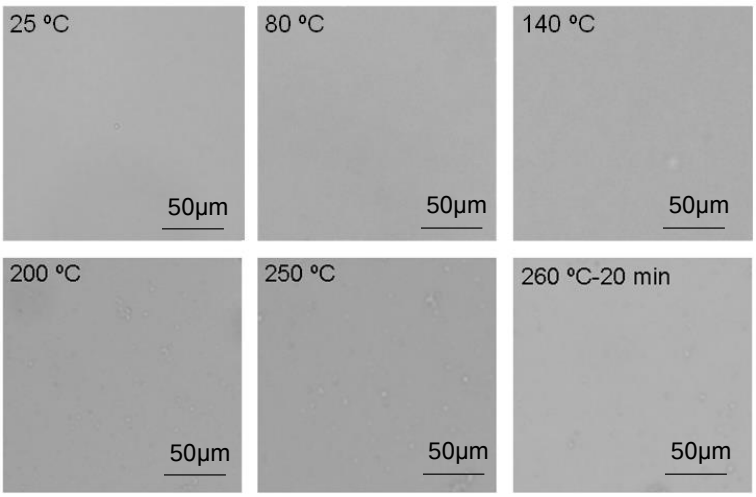

Fig. 1C

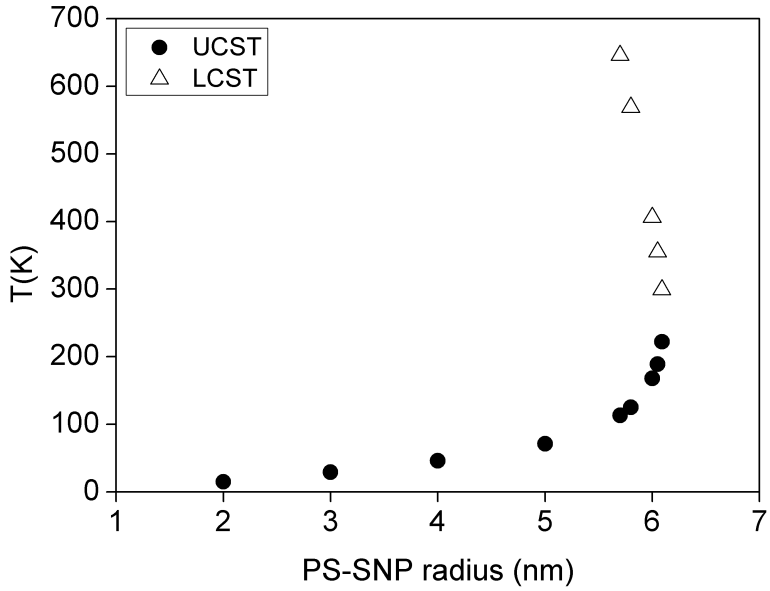

Figure 2. (TOM): Thermo-optical microscopy images of ternary PVME (M_w = 90 kDa) / PS / PS-SNP (R_p = 4 nm, cross-linking degree = 7.3 mol%) nanocomposite (PS/PVME volume

ratio = 1) thin films recorded at a scanning rate of 1 ºC/min, as a function of nanoparticle volume fraction, $\phi_{PS\text{-}SNP}$, and PS molecular weight, M_w(PS): (A) $\phi_{PS\text{-}SNP}$ = 0.05, M_w(PS) = 35 kDa, (B) $\phi_{PS\text{-}SNP}$ = 0.05, M_w(PS) = 65 kDa, (C) $\phi_{PS\text{-}SNP}$ = 0.05, M_w(PS) = 284 kDa, (D) $\phi_{PS\text{-}SNP}$ = 0.1, M_w(PS) = 35 kDa, (E) $\phi_{PS\text{-}SNP}$ = 0.1, M_w(PS) = 65 kDa, and (F) $\phi_{PS\text{-}SNP}$ = 0.1, M_w(PS) = 284 kDa. (AFM): Comparison of AFM images (height and phase) recorded after rapid quenching of PVME (M_w = 90 kDa) / PS / PS-SNP (R_p = 4 nm, cross-linking degree = 7.3 mol%) nanocomposite (PS/PVME volume ratio = 1) thin films annealed during 30 minutes at T = T_c + 10 ºC: (A) $\phi_{PS\text{-}SNP}$ = 0, M_w(PS) = 35 kDa, (B) $\phi_{PS\text{-}SNP}$ = 0.05, M_w(PS) = 35 kDa, (C) $\phi_{PS\text{-}SNP}$ = 0, M_w(PS) = 65 kDa, (D) $\phi_{PS\text{-}SNP}$ = 0.05, M_w(PS) = 65 kDa, (E) $\phi_{PS\text{-}SNP}$ = 0, M_w(PS) = 284 kDa, and (F) $\phi_{PS\text{-}SNP}$ = 0.05, M_w(PS) = 284 kDa. T_c, the cloud-point temperature, was determined by thermo-optical microscopy.

Fig. 2 TOM

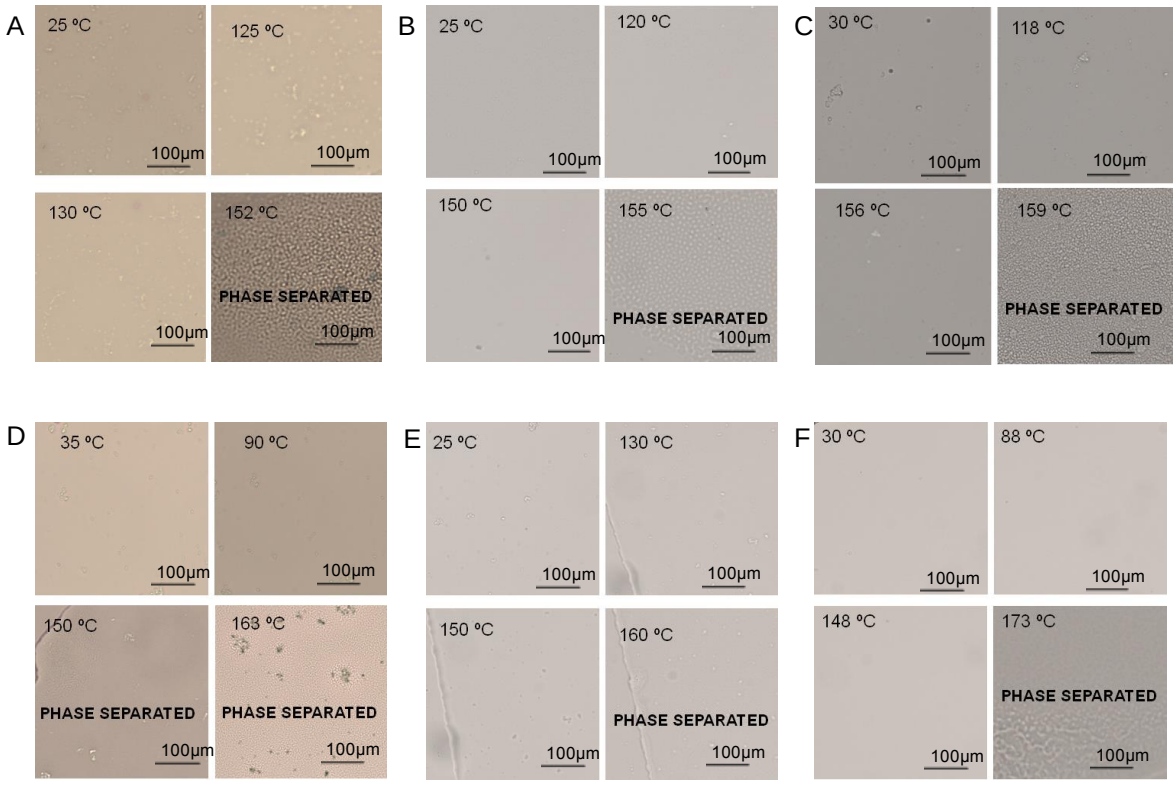

Fig. 2 AFM

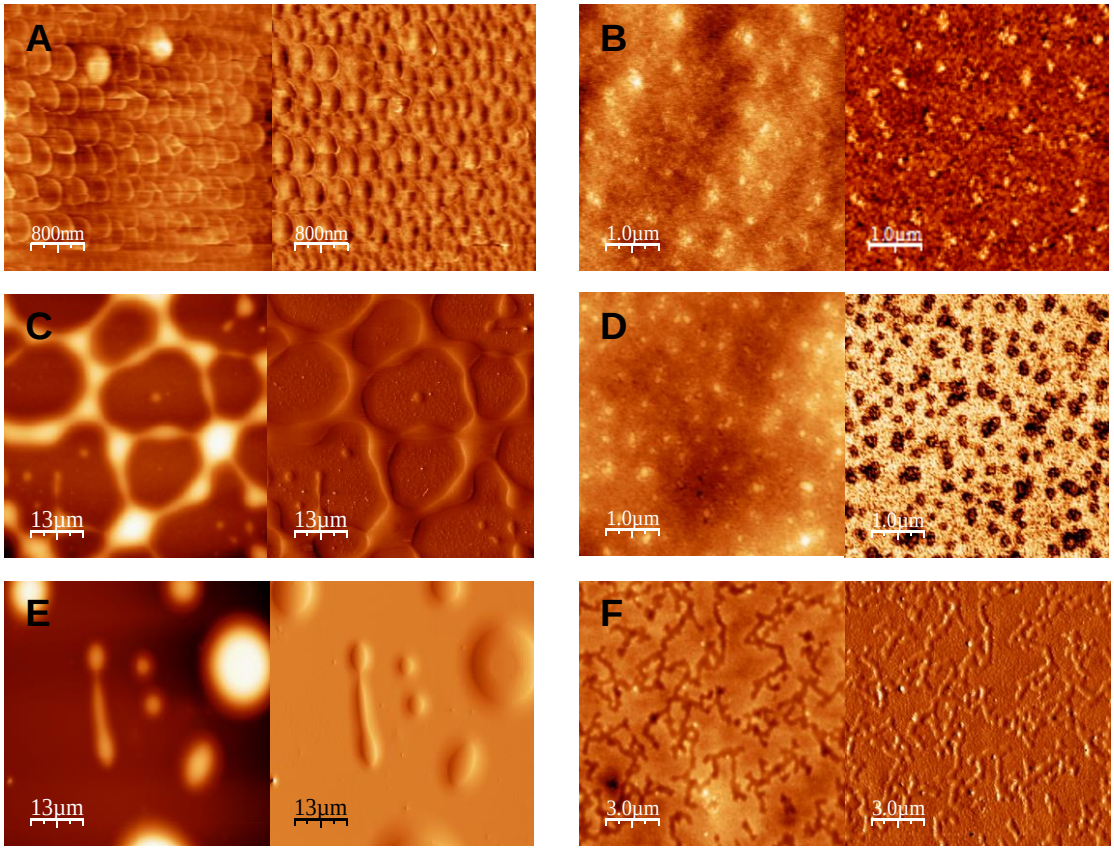

Figure 3. Estimation of the phase separation temperature for PVME (M_w = 90 kDa) / PS (M_w = 35 kDa) / PS-SNP (R_p = 4 nm, cross-linking degree = 7.3 mol%) nanocomposites

(PS/PVME volume ratio = 1) from rheological measurements in the linear regime by means of a $\Gamma \equiv \left[\frac{(G'')^2}{G'T} \right]^{2/3}$ versus 1/T plot for: (A) $\phi_{PS\text{-}SNP}$ = 0, (B) $\phi_{PS\text{-}SNP}$ = 0.05, and (C) $\phi_{PS\text{-}SNP}$ = 0.1. $\phi_{PS\text{-}SNP}$ is the volume fraction of PS-SNP in the nanocomposite, G´ is the elastic modulus, G´´ is the loss modulus and T is the absolute temperature. (D) Comparison of theoretical spinodal phase separation temperatures calculated from a thermodynamic model for ternary PVME / PS / PS-SNP soft nanocomposites (see Supplementary Information) and experimentally determined phase separation temperatures by thermo-optical microscopy (T_c, open symbols) and rheological measurements (T_s, filled symbols), as a function of PS molecular weight (M_w,PS = 35 kDa, circles; M_w,PS = 65 kDa, squares; and M_w,PS = 284 kDa, triangles) and composition ($\phi_{PS\text{-}SNP}$ = 0, blue; $\phi_{PS\text{-}SNP}$ = 0.05, green; and $\phi_{PS\text{-}SNP}$ = 0.1, red). Model parameters employed in the calculations were taken directly from reference [40].

Fig. 3A

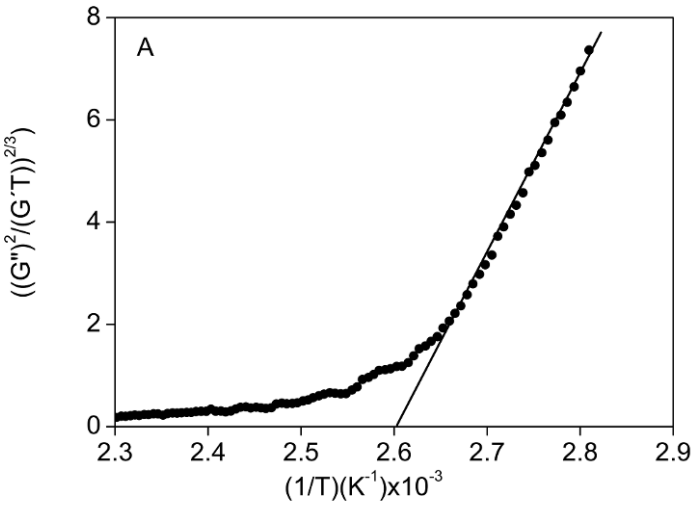

Fig. 3B

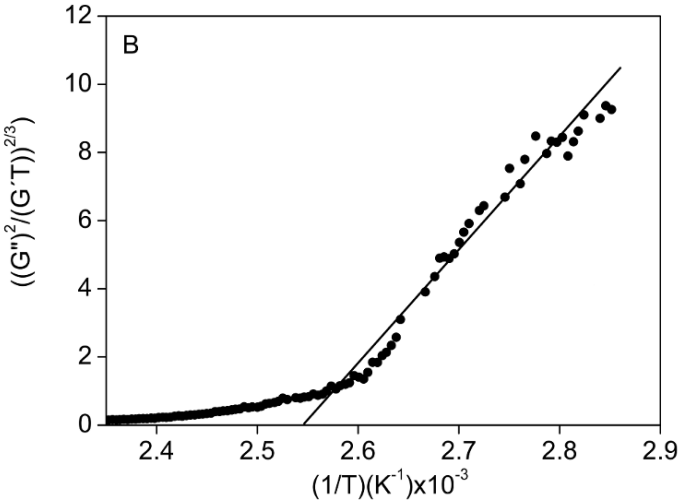

Fig. 3C

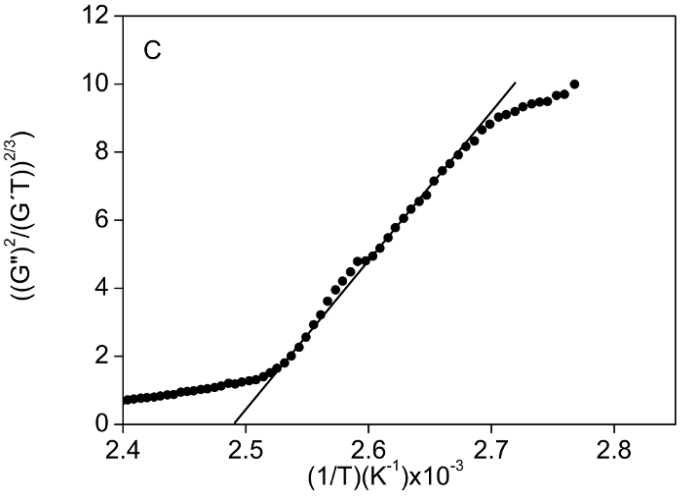

Fig. 3D

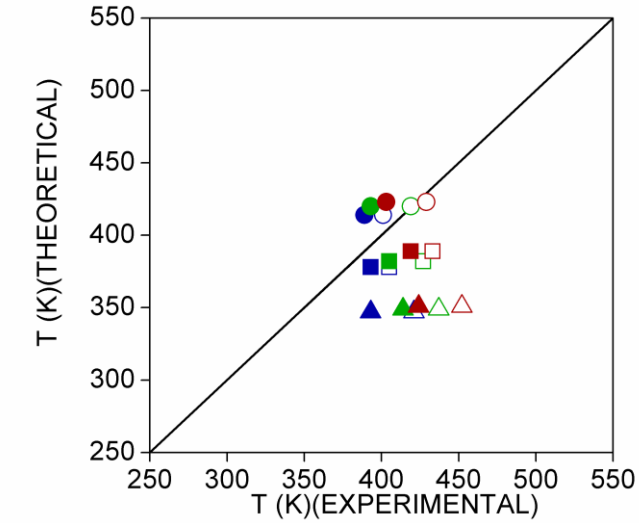

DOI: 10.1002/marc.201000720
Article Type: Communication

A promising Nanotechnology pathway: First experimental evidence of arrested phase separation in soft nanocomposites involving ultra-small, unimolecular nanoparticles paves the way to nanocomposite materials with excellent nanoparticle dispersion across a broad temperate range.

José A. Pomposo*, Alaitz Ruiz-de-Luzuriaga, Iñaki García, Agustín Etxeberria, Juan Colmenero

A Nanotechnology Pathway to Arresting Phase Separation in Soft Nanocomposites

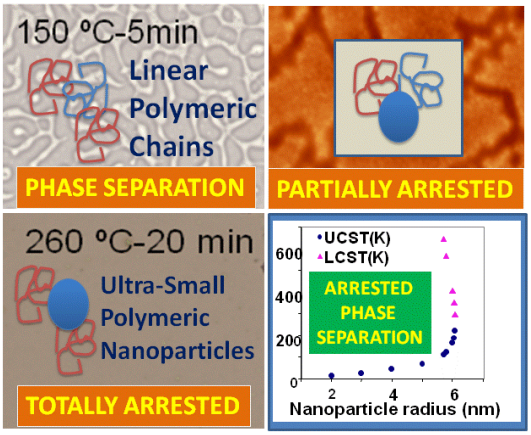

Macromolecular Rapid Communications
DOI: 10.1002/marc.201000720

Supporting Information

A Nanotechnology Pathway to Arresting Phase Separation in Soft Nanocomposites

José A. Pomposo*, Alaitz Ruiz de Luzuriaga, Iñaki García, Agustín Etxeberria, Juan Colmenero

A. TGA curves of PS-SNPs and PVME pure materials

Significant PVME thermal degradation is observed in **Figure S1B** at temperatures above 200 ºC.

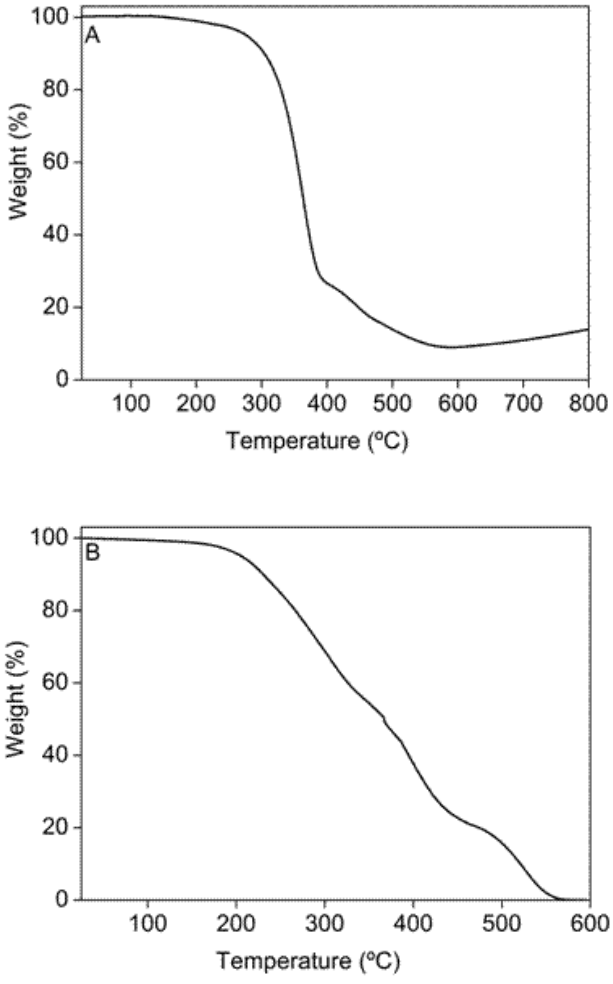

Figure S1. Weight loss *versus* temperature curves of (A) PS-SNPs and (B) PVME recorded under nitrogen atmosphere at a heating rate of 1 ºC/min. R_p(PS-SNP) = 4 nm and M_w (PVME) = 90 kDa.

B. AFM images of binary PS-SNPs / PVME nanocomposite films annealed at high temperature

The presence of bubbles across the film arising from PVME thermal degradation is clearly seen in the AFM picture, but no sign of phase-splitting is observed.

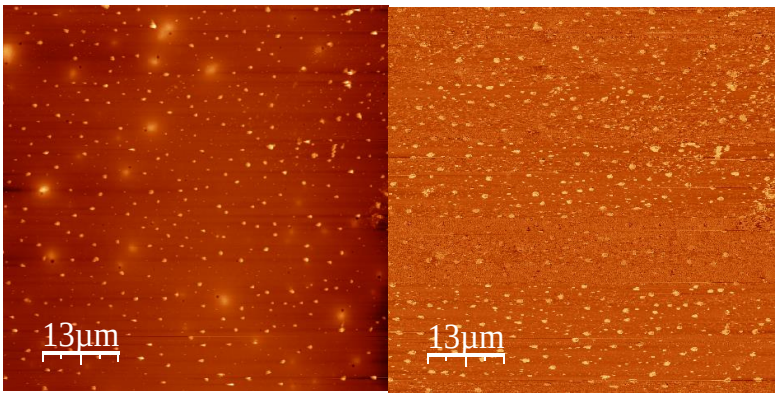

Figure S2. AFM pictures of binary PS-SNPs (R_p = 4 nm) / PVME (M_w = 90 kDa, ϕ_{PVME} = 0.8) nanocomposite films recorded after isothermal annealing during 30 min. at T_a= 240 ºC and rapid quenching to room temperature.

C. TOM images of binary PS / PVME (1/1) blends and ternary PS / PVME (1/1) / PS-SNPs nanocomposites annealed at high temperature

Slow-down kinetics in the ternary all-polymer nanocomposite is clearly observed by comparing Figure S3A-B and Figure S3C-E.

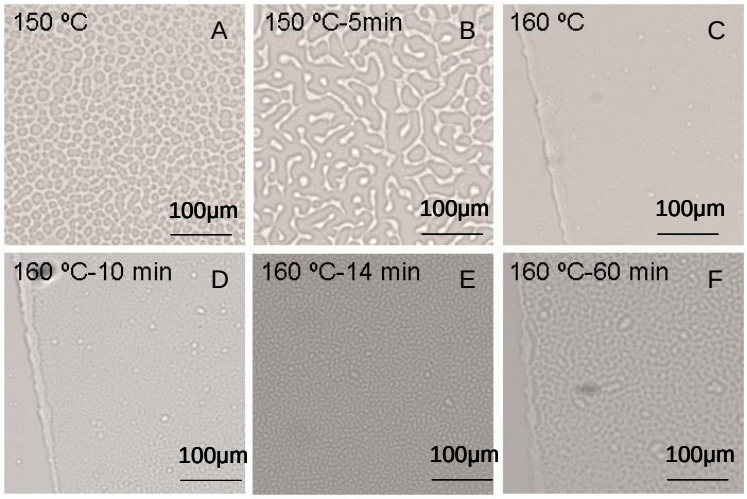

Figure S3. TOM pictures of binary PS / PVME (1/1) blends recorded at 150 ºC (A), at 150 ºC after isothermal annealing for 5 min. (B), and ternary PS (M_w = 65 kDa) / PVME (M_w = 90 kDa) (1/1) / PS-SNPs (R_p = 4 nm, $\phi_{PS\text{-}SNP}$ = 0.1) nanocomposites recorded at 160 ºC (C), and at 160 ºC, after isothermal annealing at such temperature for 10 min. (D), 14 min. (E), and 60 min. (F).

D. Phase-splitting in binary PS / poly(styrene$_{0.84}$-co-azidomethyl styrene$_{0.075}$-co-2-methyl-acrylic acid 3-trimethylsilanyl-prop-2-ynyl ester$_{0.076}$) blends

The miscibility improving effect in PVME/PS-SNPs blends is indeed induced by the so called weakly interaction of ultra-small nanoparticles and not by the higher polarity of PS component in the blend, since PVME / linear-poly(styrene$_{0.84}$-co-azidomethyl styrene$_{0.075}$-co-2-methyl-acrylic acid 3-trimethylsilanyl-prop-2-ynyl ester$_{0.076}$) blends shows phase-splitting (LCST-type) at temperatures above T_c = 144 ºC. T_c for conventional PVME / linear-PS blends of similar molecular weights was 135 ºC.

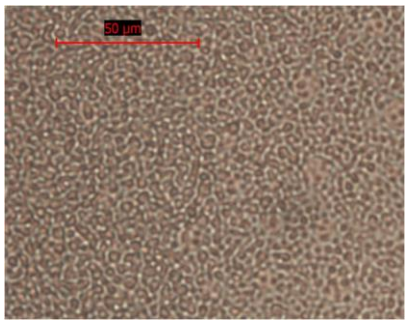

Figure S4. TOM image of a binary PS / linear-poly(styrene$_{0.84}$-co-azidomethyl styrene$_{0.075}$-co-2-methyl-acrylic acid 3-trimethylsilanyl-prop-2-ynyl ester$_{0.076}$) (1/1) blend recorded at 144 ºC. Scanning rate during TOM measurements was 1 ºC/min.

E. Thermodynamic model for predicting the phase behavior of ternary soft nanocomposites

Here we present an extension of the compressible regular solution free energy model recently introduced for describing the phase behavior of binary soft nanocomposites. A detailed description of the theoretical approach employed is provided in reference [1] and the foundations of the compressible "regular" solution theory in reference [2]. In brief, the free energy of the system at atmospheric pressure is given by:

$$F_m = F_m^{co} + F_m^{np-np} + F_m^{\text{int}} + F_m^{np-p} \tag{S1}$$

For ternary all-polymer nanocomposites, the first term accounting for the changes in combinatorial free energy of the system is just given by:

$$F_m^{co} = kT\left[\frac{\phi_A\hat{\rho}_A}{\nu_p}\ln\phi_A + \frac{\phi_B\hat{\rho}_B}{N_B\nu_B}\ln\phi_B + \frac{\phi_C\hat{\rho}_C}{N_C\nu_C}\ln\phi_C\right] \tag{S2}$$

where ϕ_i, ρ_i, ν_i and N_i are, respectively, the volumen fraction, mass density, hard-core volume and segment number of component i, and ν_p is the nanoparticle volume (component A) at temperature T.

The second term in eq. S1 shows the change in interaction energy upon mixing non-rigid polymer-nanoparticles and linear-polymer chains (components B and C) according to the compressible version of the "regular" solution theory:

$$F_m^{\text{int}} = (\hat{\rho}_B\phi_B)(\hat{\rho}_C\phi_C)(\delta_{B,0}-\delta_{C,0})^2 + (\phi_B\phi_C)(\hat{\rho}_B-\hat{\rho}_C)(\delta_B^2-\delta_C^2)$$
$$+\frac{r_B}{R_p}\left[(\hat{\rho}_B\phi_B)(\hat{\rho}_A\phi_A)(\delta_{B,0}-\delta_{A,0})^2 + (\phi_B\phi_A)(\hat{\rho}_B-\hat{\rho}_A)(\delta_B^2-\delta_A^2)\right]$$
$$+\frac{r_C}{R_p}\left[(\hat{\rho}_C\phi_C)(\hat{\rho}_A\phi_A)(\delta_{C,0}-\delta_{A,0})^2 + (\phi_C\phi_A)(\hat{\rho}_C-\hat{\rho}_A)(\delta_C^2-\delta_A^2)\right] \quad \text{(S3)}$$

where $\delta_{i,0}^2$ and δ_i^2 are the hard-core and the T-dependent energy densities of component i, respectively, r_i the monomer radius of component i and R_p the nanoparticle radius.

The third term in eq. S1 gives the contribution to the free energy of mixing arising from non-ideal entropic nanoparticle-nanoparticle contributions. Specifically, it gives the change in free energy experienced by the nanoparticles on going from the neat fluid state to the mixed state:

$$F_m^{np-np} = kT\left(\frac{\phi_A\hat{\rho}_A}{v_p}\right)\left(\frac{4\phi_A-3\phi_A^2}{(1-\phi_A)^2}\right) \quad \text{(S4)}$$

As reported previously, the neat change in free energy is favorable to mixing due to the dilution of short-range contact nanoparticle-nanoparticle interactions. This effect is geometric in nature as a consequence of the relative compact nature of the nanoparticles.

Finally, the fourth term in eq. S1 includes the contribution to the free energy of mixing arising from the stretching of the linear-polymer chains due to the presence of the nanoparticles in terms of a "universal" Ginzburg-type expansion term insensitive to the chemical nature of the components but dependent on chain length and nanoparticle size:

$$F_m^{np-p} = kT\left(\left[\frac{3}{2}\frac{\phi_A\phi_B\hat{\rho}_A\hat{\rho}_B}{N_Bv_B}\left(\frac{R_p}{R_{gB}}\right)^2\right]+\left[\frac{3}{2}\frac{\phi_A\phi_C\hat{\rho}_A\hat{\rho}_C}{N_Cv_C}\left(\frac{R_p}{R_{gC}}\right)^2\right]\right) \quad \text{(S5)}$$

It is significant that equations S1-S5 can be used (in conjunction with equation 3 in the manuscript corresponding to the spinodal phase boundary) in a *predictive* way by using pure component parameters previously compiled by Ruzette *et al.* (Table 1 in Ref. [2] and Table 1 in Ref. [3]). In this sense, the corresponding expressions for the second derivatives of the free energy with respect to composition (at constant temperature, pressure and reduced density) are:

$$\frac{\partial^2 F_m}{\partial \phi_A{}^2} = kT\left[\frac{\hat{\rho}_A}{\upsilon_p \phi_A} + \frac{\hat{\rho}_C}{N_C \upsilon_C (1-\phi_A-\phi_B)}\right]$$
$$-2\left(\frac{r_C}{R_p}\right)\left[(\hat{\rho}_C\,\hat{\rho}_A)(\delta_{C,0}-\delta_{A,0})^2 + \left(\hat{\rho}_C - \hat{\rho}_A\right)\left(\delta_C^2-\delta_A^2\right)\right]$$
$$+kT\left[2\times\frac{\hat{\rho}_A}{\upsilon_p}\left(\frac{4-\phi_A}{(1-\phi_A)^4}\right) - 3\times\frac{\hat{\rho}_A\,\hat{\rho}_C}{N_C\upsilon_C}\left(\frac{R_p}{R_{g,C}}\right)^2\right] \quad \text{(S6)}$$

$$\frac{\partial^2 F_m}{\partial \phi_B{}^2} = kT\left[\frac{\hat{\rho}_B}{N_B\upsilon_B\phi_B} + \frac{\hat{\rho}_C}{N_C\upsilon_C(1-\phi_A-\phi_B)}\right] - 2\left[(\hat{\rho}_B\,\hat{\rho}_C)(\delta_{B,0}-\delta_{C,0})^2 + \left(\hat{\rho}_B-\hat{\rho}_C\right)\left(\delta_B^2-\delta_C^2\right)\right] \quad \text{(S7)}$$

$$\frac{\partial^2 F_m}{\partial\phi_A\partial\phi_B} = \frac{\partial^2 F_m}{\partial\phi_B\partial\phi_A} = kT\left[\frac{\hat{\rho}_C}{N_C\upsilon_C(1-\phi_A-\phi_B)}\right] - \left[(\hat{\rho}_B\,\hat{\rho}_C)(\delta_{B,0}-\delta_{C,0})^2 + \left(\hat{\rho}_B-\hat{\rho}_C\right)\left(\delta_B^2-\delta_C^2\right)\right]$$
$$+\left(\frac{r_B}{R_p}\right)\left[(\hat{\rho}_B\,\hat{\rho}_A)(\delta_{B,0}-\delta_{A,0})^2 + \left(\hat{\rho}_B-\hat{\rho}_A\right)\left(\delta_B^2-\delta_A^2\right)\right]$$
$$-\left(\frac{r_C}{R_p}\right)\left[(\hat{\rho}_C\,\hat{\rho}_A)(\delta_{C,0}-\delta_{A,0})^2 + \left(\hat{\rho}_C-\hat{\rho}_A\right)\left(\delta_C^2-\delta_A^2\right)\right]$$
$$+\frac{3}{2}kT\left[\frac{\hat{\rho}_A\,\hat{\rho}_B}{N_B\upsilon_B}\left(\frac{R_p}{R_{g,B}}\right)^2 - \frac{\hat{\rho}_A\,\hat{\rho}_C}{N_C\upsilon_C}\left(\frac{R_p}{R_{g,C}}\right)^2\right] \quad \text{(S8)}$$

References:

1. A. Ruiz de Luzuriaga, H. J. Grande, J. A. Pomposo, *J. Chem. Phys.* **2009**, *130*, 084905.
2. A.-V. G. Ruzette, A. M. Mayes, *Macromolecules* **2001**, *34*, 1894.
3. J. A. Gonzalez-Leon, A. M. Mayes, *Macromolecules* **2003**, *36*, 2508.